International Journal of Thin Films Science and Technology

http://dx.doi.org/10.18576/ijtfst/120207

Synthesis of a Novel Approach of Fabricating Tin Oxide Nanostructures Thin Film for Industrial Applications

Hyacinth K. Idu[1,*], *Majeed Amini*[2] *and Christian A. Elekwa*[3]

[1]Physics Department, Faculty of Science, Taraba State University, Jalingo, Nigeria
[2]College of Arts and Science, Ahlia University, Manama, kingdom of Bahrain
[3]Industrial Physics Department, Faculty of Science, Ebonyi State, Abakaliki, Ebonyi State

Received: 22 Feb. 2023, Revised: 23 Mar. 2023, Accepted: 12 Apr. 2023
Published online: 1 May 2023

Abstract: Biphasic nanocomposites consisting of tin oxide (SnO) are of great interest to the research community due to their potential use in various optoelectronic devices. In this paper, SnO and SnO/Zn nanostructures were explored using spray pyrolysis techniques. Diffractometric and spectrometric methods were employed to examine the optical characteristics and elemental composition of the deposited thin films. The XRD data showed that the deposited thin films were polycrystalline. The diffractograms of biphasic films of SnO/ZnS showed lower intensity compared to uncoated SnO samples, regardless of the substrate temperature. The absorbance of SnO thin films varied between 0.10 and 0.7 at different substrate temperatures, while the absorbance of biphasic films of SnO/ZnS changed depending on the substrate temperature. The reflectance spectra of SnO films showed fluctuations between maxima and minima, whereas biphasic films had low reflectance. The band gap of biphasic films was between 1.30 eV and 1.10 eV for different substrate temperatures, indicating their suitability for use due to the rise in SnO/ZnS bandgap. The extinction coefficient (k) of SnO films increased with increasing substrate temperature, while biphasic films showed a significant reduction in magnitude, irrespective of the substrate temperature. The refractive index of the film samples was generally low, regardless of the substrate temperature. The study discussed the potential applications of the thin films and found good agreement with experimental data.

Key Words: Tin Oxide, SnO/ZnS, transmittance, reflectance, refractive index(n), absorbance, band gap (Eg) , Spray pyrolysis technique and XRD

1 Introduction

Due of their practical applications in numerous fields, biphasic nanostructured materials on a nanoscale scale have attracted the attention of many researchers in recent years. These components exhibit unique properties arising from the combination of SnO and coating materials in their geometric or designed form [1,2].

More specifically, they have been created so that the coating material can increase the SnO-structured material's oxidation stability, thermal stability, or surface reactivity. The coating materials are significant because they have the potential to affect the charge, functionality, and dispersiveness of SnO structured materials [3,4]. The researchers were interested in depositing SnO/TMC-type biphasic structured materials. As a result, we would be able to create thin films that combine the special qualities of transition metals and tin oxide, making them viable materials for window layers in heterojunction/CIGS solar cells, photonic devices, and other applications. The study of oxide thin-film materials has drawn a lot of attention as one of the most alluring areas of study for physicists and material scientists. Many applications in semiconductor devices, such as optoelectronic and solar energy devices, have continued to draw significant attention to the research of tin oxide thin films coated with transition metal chalcogenides in various substrates.

Tin oxide's growth resistance on a variety of substrates depends on the development of a compact, adherent passive oxide coating [5-7]. As a result, the fabrication of a wide variety of electronic devices in modern industry typically uses thin films of various metal oxides. They are used in electronic devices as fundamental components for a variety of purposes, including optical devices for UV-visible

*Corresponding author E-mail: iduhyacinthkevin@gmail.com

spectral area applications, colored layers, solar cells/collectors, automotive parts, barriers, and insulating layers. Regarding performance and durability, these applications offer special advantages [8–10]. Therefore, this research work is focused on the synthesis of a novel approach of fabricating tin oxide (SnO) nanostructures thin film for industrial applications. These composite thin films deposited were characterized to ascertain their structure, optical and solid state properties for possible application in engineering, science and technology.

2 Experimental details

2.1. Materials used.

The materials used are; soda lime glass substrates, synthetic foam, beakers, thermometer, digital (PH meter) type (Inolab PH720), automatic magnetic stirrer, distilled water, Thiorea (SC(NH2))2, aqueous ammonia (NH4OH), ammonia (NH3), tin oxide (SnO), zinc chloride (ZnCl2) acetone, and other source materials that are deemed necessary. All the source chemicals used for the deposition of the SnO thin films and the doped films were of analytical grade, obtained from Testbourne Chemical Limited, and Sigma Aldrich, all from UK through local suppliers.

2.2. Substrate preparation

The Microscopic glass slide or substrate of area 26 mm x 76mm, the thickness of 1.0 mm,and refractive index of 1.52 were used and thoroughly washed using detergent and distilled water. The washed slide was soaked in methanol for 1 hour and rinsed in distilled water, after which the slides were then oven-dried at a temperature of 60 0C. The degreased and cleaned surfaces of substrate enhance better nucleation of thin films growth.

2.3. Synthesis of SnO and SnO/ZnS thin films

The same growth conditions were used to prepare both SnO and SnO/ZnS simultaneously. Initially, 40 ml of 0.1 M solutions of zinc chloride (ZnCl2), sodium hydroxide (NaOH), and thiourea (NH2CSNH2) in a ratio of 5:5 and 4 drops of ammonia (NH3) solution were combined in a beaker to create zinc sulphide (ZnS). In order to improve the mixture, a magnetic stirrer was used for 30 minutes to create a homogeneous solution. Following stirring, 10 ml was measured out using a pump syringe into a sample bottle that was positioned on nozzle value and sprayed on a heated substrate/slide of SnO films that had already been deposited at 100 oC temperature. At 150 oC and 200 oC, respectively, these were repeated for two separate 10 ml of the solution. The following characteristics were measured during the deposition process: substrate temperature, deposition time, nozzle air pressure, deposition angle, deposition distance, and height. The most crucial element in the deposition of SnO (core) thin-films and SnO/ZnS biphasic thin films was the substrate temperature. This is because droplet drying, breakdown processes, crystallization, and thin-film formation are all influenced by the substrate temperature.

2.4. Determinations of film thickness

The behavior of the majority of semiconductor thin film materials is largely determined by one of the fundamental and important characteristics, film thickness. The software Sem.Afore 5.2.1 was used in this investigation to determine the film thickness.

2.5 Characterization methods

X-ray A DW-XRD-Y3000 Model was used to carry out the difraction on the thin films, and the crystal structures of the films were identified from the XRD peaks. For comparative purposes, the XRD was conducted on each sample using a continuous scan mode with a 2=100–700 scanning range. Using an Agilant Technologies Cary 60 UV-Vis spectrometer with an 800 to 300 nm wavelength range, the optical characteristics of the thin films were measured. The baseline was adjusted for all of the spectral data.

3 Results

3.1 X-ray diffraction (XRD) analysis

The X-ray diffraction (XRD) method was used to examine the structure of the SnO thin films. The diffraction spectra were measured at angle 2θ (scanning the diffraction angle from 0 to 90o deepens with CUK radiation λ = 1.54060 nm). Figures 1A to 1B display the deposited films' XRD patterns. As-deposited in Figure 1A, SnO thin films with somewhat different thicknesses were put to glass at varied substrate temperatures. Peak broadening, which was employed to ascertain the bandgap energy, captured the diffraction pattern of the crystalline thin films in accordance with the findings of the optical properties as shown in the graph. The peak broadening caused by the quantum size effect might be attributed to a phase transition that took place in a deposition at substrate temperatures of 100°C, 150°C, and 200°C. Another explanation for the peak broadening is the high melting point of tin and the fact that the thin films were not completely oxidized at these deposition temperatures (232oC). The inter-planar distance, or d, is measured using XRD patterns with distinct diffraction peaks that represent the (111), (200), and (101) lattice planes. These patterns imply that the substrate temperature maxima are increasing [19]. Peak broadening in the crystalline films is shown in the XRD pattern of SnO/ZnS films that were formed on various substrate temperatures. The research showed that the SnO/ZnS films are polycrystalline in nature. With low reflection peaks at (110), (114), and (105) planes, the observed diffraction peaks at 2θ values of 37.6o, 20o, and 35o, respectively, correspond to (101), (112), and (211) planes. The interface between the SnO and ZnS atoms in the lattice of SnO/ZnS and the non-uniformity in the evaporation process during the time of deposition may be responsible for the observed variation difference of the peaks.

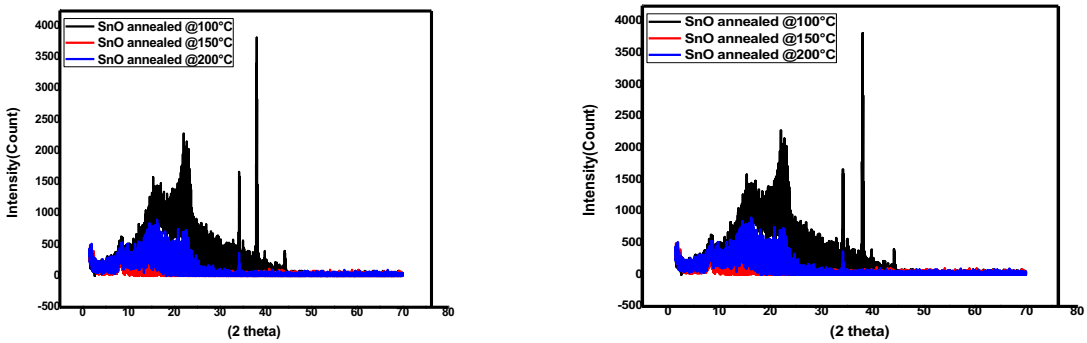

Fig. 1: XRD pattern of: (A) as-deposited SnO and (B) SnO/ZnS thin film

3.2 UV-Vis spectral Analysis

The experimental results from these studies, which included measurements of absorbance, transmittance, reflectance, refractive index, extinction coefficient, and bandgap at different substrate temperatures, are shown in Figures 1 to 6. The UV-visible transmittance spectrum for SnO thin films and SnO/ZnS biphasic thin films, both of which were created at different substrate temperatures, is displayed in Figures 2A and B. All SnO thin films and biphasic thin films have high transmittance (> 95%) in the visible region of the solar spectrum, as can be seen in the illustration. All prepared SnO thin films and all biphasic films have relatively high transmission, however the transmission band edge is where it abruptly drops off. This is explained by the excellent homogeneity of the thin films created during the deposition. Similar preparations have been documented in recent research using CuS core-shell [14–17].

At different substrate temperatures, as depicted in Fig. 3 (A-B), the absorbance of SnO and SnO/ZnS lowers by around 300–350 nm, increases by 350–500 nm, and then decreases by 500–900 nm. This might have occurred because the thin film's wavelength was reduced as a result of the substrates' homogeneous absorption of the generated oxide layer. The SnO/ZnS composite's average absorption was lower than that of the core SnO, though. This demonstrates that the absorbance spectrum of the SnO (core) thin film was changed during the development of the SnO/ ZnS composites. Moreover, SnO. TMCs (SnO/ZnS) composites from the plot showed that they absorbed more successfully in the visible region compared to other regions. Due to these characteristics, the films can be employed as coating materials for anti-reflective, eyeglass, and solar.

For the SnO and SnO/ZnS biphasic thin films formed in this investigation, Fig. 4(A-B) shows a plot of reflectance against wavelength. The reflectance of the entire SnO thin film was between 300 and 350 nm in the visible area. From there, the reflectance decreased sharply between 350 and 500 nm, then gradually between 500 and 900 nm. The reflectance of the biphasic thin film is seen from the figures. This results in a sudden decrease in reflectance and a subsequent sharp increase in wavelength. At 500 nm of wavelength, the rate of reflectance growth was highly rapid before slowing down later. This proved that the synthesis of biphasic SnO/ZnS composites had significantly altered the reflectance of the spectra of the SnO component. The biphasic thin films had the lowest reflectance value, 20%, while the core SnO thin film had the highest recorded reflectance value of > 96%. A reflectance rating of less than 20% is ideal for sola control glazing to avoid glare problems. They can be employed as temperature control coatings and antireflection coatings because of their outstanding transparency over the whole visible spectrum.

The biphasic SnO/TMC thin films' low reflectance may have been caused by high transmittance and a high refractive index. [22-24].Figure 5 depicts the refractive index as a function of photon energy for both the biphasic SnO/ZnS thin films and the deposited SnO thin films. The SnO thin film's maximum refractive index, which is about 1.22, is remarkably similar to what was discovered by [25]. The graphs demonstrate that when SnO thin films are

coated with ZnS, which affects the refractive index, the refractive index value of the biphasic thin films increases by 1.44. From the figure, we inferred that, with the exception of a place where the refractive index rises as photon energy rises, the refractive index value of biphasic thin films tends to fall as photon energy rises. The thin-film oxide was responsible for the substrate's highest performance, which was seen.

Figure 6 depicts the relationship between the extinction coefficient and photon energy for biphasic and thin SnO films formed at various substrate temperatures. We noticed a steady rise in the K value as we approached greater photon energies. The plot shows that when substrate temperatures rise, the extinction coefficient falls. The outcomes showed that homogeneity was taking place and that biphasic thin films were evenly dispersed on the SnO thin film. This agrees with the findings of [26,29].

Figure 7 illustrates the relationship between the absorption coefficient and photon energy (hv) for thin films made of SnO and SnO/ZnS. (A-B). By extrapolating the linear component of the curve to the point of zero absorption coefficient from this relationship, the optical band gap may be calculated. At substrate temperatures of 100 oC, 150 oC, and 200 oC, the plot shows that the band gaps for the SnO thin

film are, respectively, 2.00 eV, 2.10 eV, and 2.20 eV. The energy bandgap of SnO thin films displayed a blue shift as the substrate temperature increased. The increase in crystalline size at substrate temperatures of 100 °C, 150 °C, and 200 °C, respectively, could account for this. According to [21,30], as the substrate temperature rises, the optical bandgap widens.The energy bandgap of the biphasic SnO/ZnS composites has a minor advantage over that of SnO, according to as-deposited SnO thin films (Fig. 7B). This is evidence that the combination of SnO and ZnS components to create a SnO/ZnS biphasic composite configuration (heterojunction) modified the SnO with the intriguing synergetic properties offered by the composites, shifting the fundamental absorption edge towards longer wavelength and resulting in a smaller bandgap.

This offers the bandgap's tuning impact for a particular application. According to the graph, the examined SnO/ZnS thin films' optical bandgap had a redshift after biphasic production, with energy bandgap values falling from 13.0 eV, 1.20 eV, and 1.10 eV. These films are perfect for use as a window layer in heterojunction solar cells, CIGS solar cells, photonic devices, photovoltaic solar cells, and other applications because of the bandgap energy they exhibit [17,18,21]. Figures 2-7 (A and B) show the observed discontinuities in the plotted graphs, which may be caused by quantum size effects [31-25] associated with the phase transition that results in a deposition at substrate temperatures of 100°C, 150°C, and 200°C [3,2].

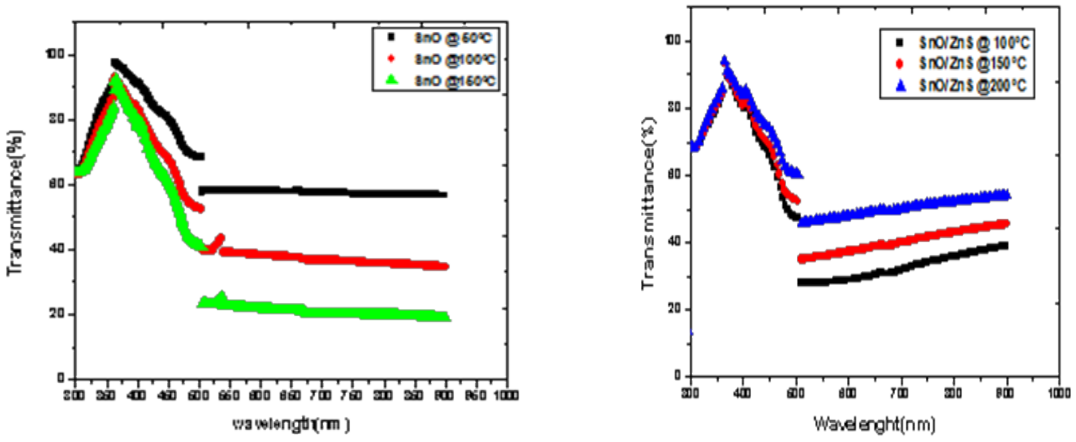

Fig. 2: Plot of transmittance against wavelength for : (A) as-deposited SnO thin film and (B) SnO/ZnS Thin film.

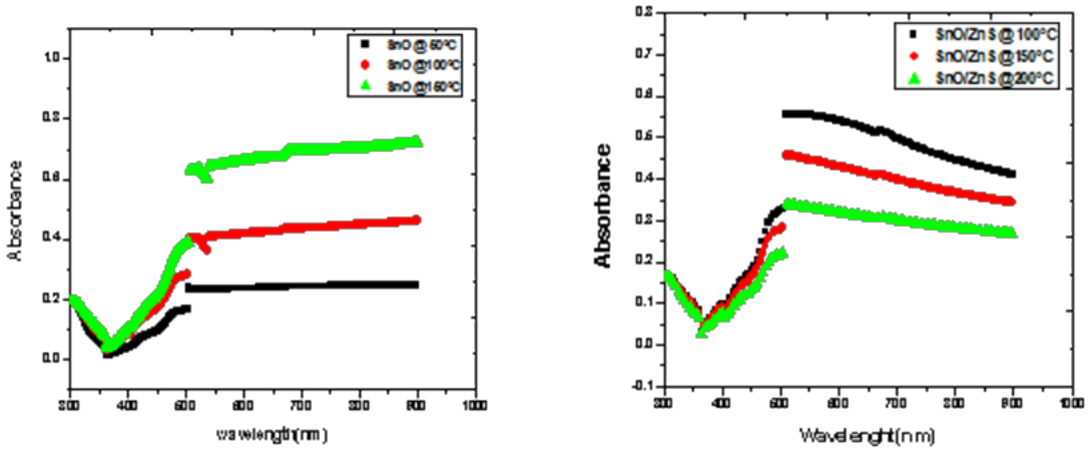

Fig. 3: Plot of absorbance against wavelength for : (A) as-deposited SnO thin film and (B) SnO/ZnS Thin film

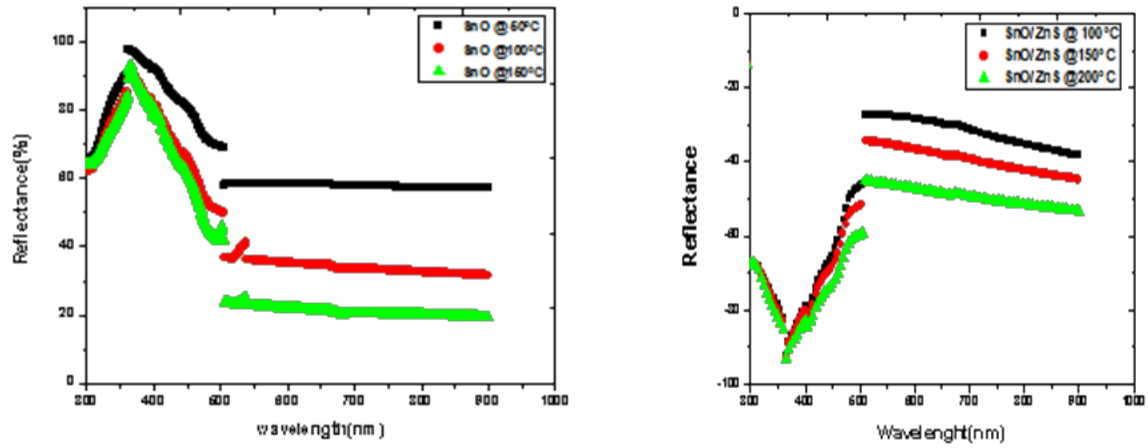

Fig. 4: Plot of reflectance against wavelength for : (A) as-deposited SnO thin film and (B) SnO/ZnS Thin film.

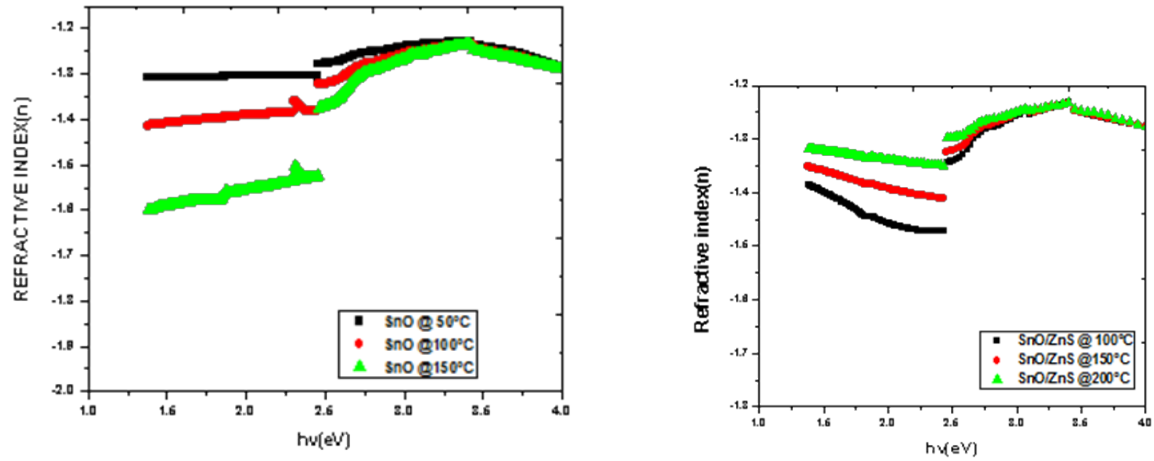

Fig. 5: Plot of refractive Index (n) against hv for : (A) as-deposited SnO thin film and (B) SnO/ZnS Thin film.

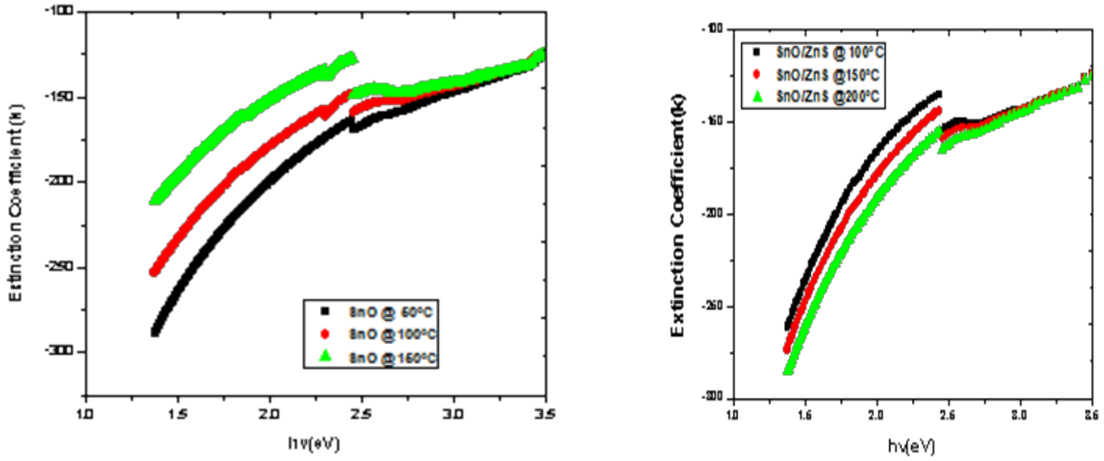

Fig. 6: Plot of ExtinctionCofficient (k) against *hv* for : (A) as-deposited SnO thin film and (B) SnO/ZnS Thin film.

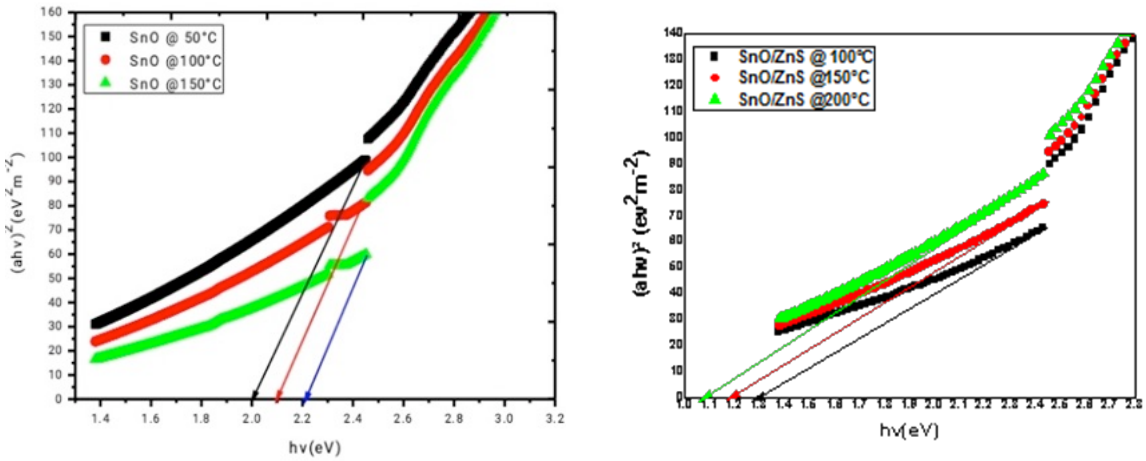

Fig. 7: Plot of against hv for : (A) as-deposited SnO thin film and (B) SnO/ZnS Thin film.

In conclusion, we have given a thorough investigation of the synthesis of the thin filme on the structural and optical characteristics of SnO/ZnS by spray pyrolysis. The optimum results for spray pyrolysis deposition of SnO/ZnS films, for solar control applications, were established. Tin oxide (SnO) thin films and biphasic nanostructured composites in the form of SnO/ZnS have been effectively deposited on glass substrates using spray pyrolysis deposition techniques at temperatures of 100 °C, 150 °C, and 200 °C. The findings shown that SnO thin films and biphasic composites (SnO/TMCs) exhibit > 90% UV-region transmittance. These characteristics make the composite materials valuable in a variety of applications, including photonics, photocatalysts, UV-photodetectors or sensors (UV light sensors/detectors), and photonics. The biphasic composite thin films' absorbance spectra revealed that they did so better in the visible range than in other regions. Due to these characteristics, the films have potential uses in coating materials, anti-reflection coating and sun control, coating eyeglasses, and the creation of solar cells.

Acknowledgements

The authors acknowledge the contributions of the technical staff of the Centre for Energy Research and Development,

Obafemi Awolowo University, Ile-Ife, Osun State, Nigeria, in performing the characterisations.

References

[1] M. Ayan and M. Partha, Characterization of Sn doped ZnS thin films synthesized by chemical bath deposition technique, *Materials Research,* **20**, 430-435(2017).

[2] N. I. Ben, N. Kamoun and C. Guash, Physical properties of ZnS thin films prepared by chemical bath deposition, *Applied Surface Science*, **234**, 5039-43(2008).

[3] P. E. Agbo Refractive index and dielectric properties of TiO_2/CuO-shell thin films, *Journal of Chemistry and Materials Research*, **6,** 68-74 (2014).

[4]V.M. Pradeepa and K. Kesavan, Preparation & characterization of cus thin films via spray pyrolysis technique for photovoltaic applications, *Materials science and engineering,* **1070**, 012006 (2022).

[5] R. S. Meshram and R. M. Thombre, Optical properties of cus thin films prepared by spray pyrolysis technique at 300^0C temperature. *International Journal of Recent Scientific Research Research* , **12**, 43127-43129 (2021).

[6] K. Salim and M. N. Amroun, Improved physical properties of zno films with a second superposed sno2 very thin films deposited by s pray pyrolysis method, *Int. J. Thin. Film. Sci. Tec.,* **11**, 29-35(2022)

[7] A. Ouhaibi, M. Ghamnia, M. N. Dahamni, V. Heresanu, C. Fauquet and D. Tonneau, The effect of strontium doping on structural and morphological properties of ZnO nanofilms synthesized by ultrasonic spray pyrolysis method, *Journal of Science: Advanced Materials and Devices,* **3,** 29-36 (2018).

[8] J. Seo and H. Yoo, Zinc–tin oxide film as an earth-abundant material and its versatile applications to electronic and energy materials, *Membranes,* **12**, 1-19 (2022).

[9] K. D. Getnet, M. David, R. Laetitia, D. Jean-Luc, A. Klein, J. Carmen, D. Bellet, SnO_2 films deposited by ultrasonic spray pyrolysis: Influence of al incorporation on the properties, *Molecules,* **24,** 2797 (2019).

[10] K. Jenifer, S. Arulkumar, S. Parthiban and J. Y. Kwon, A review on the recent advancements in tin oxide-based thin-film transistors for large-area electronics, *Journal of Electronic Materials*, **49** 7098–7111 (2020).

[11] R. Sreekrishna, S. Karthik, N. S. Roshima, V. Rakhesh, *Structural and electrical properties of tin oxide films deposited by SILAR and spin coating techniques*, AIP Conference Proceedings, 2162, 020137 (2019).

[12] C. Y. Huang, L. K. Xiao, Y. H. Chang, L. Y. Chen, G. T. Chen and M. H. Li M, High-performance solution-processed Zn/SnO metal-semiconductor-metal ultraviolet photodetectors via ultraviolet/ozone photo-annealing, *Semicond. Sci. Technol.,* **36,** 095013 (2021).

[13] F. M. Ciro, A. A. Migreal and G. H. Manuel, Spray Pyrolysis techniques High-K Dietetic films and luminescent materials: A review development ode fisica, *INVESTAN*, **615,** 756-772 (2018).

[14] N. Fathy, R. Kobayashi and M. Ichimura, Preparation of ZnS thin films by pulsed electrochemical deposited, *Materials Science and Engineering* , **107**, 271-6 (2014).

[15] H. U. Igwe, and E.I.Ugwu, Optical characterization of nanocrystalline thermal annealed tin oxide thin film samples prepared by chemical bath deposition technique, *Advances in Applied Science Research*, **1,** 240-246 (2010).

[16] D. Maring, M. Cristain, M. Adriana and P. Gabriel, Zn/F-doped tin oxide nanoparticles synthesized by laser pyrolysis: structural and optical properties, *Beilstein J. Nanotechnol.,* **10,** 9-21 (2019).

[17] G. E. Patil, D.D. Kajale, V. Gaikwad and G. H. Jain, Spray pyrolysis deposition Of nanostructure tin oxide thin films, *International Scholarly Research Network*, **4,** 2-5 (2012).

[18] J. Dou, X. Li, Y. Li, Y. Chen and M. Wei, Fabrication of Zn2SnO4 microspheres with controllable shell numbers for highly efficient dye-sensitized solar cells, Sol. Energy, **181**, 424–429 (2019).

[19] Y. C. Chen, T. C. Chang, H. W. Li, W. F. Chung, C. P. Wu, S. C. Chen, J. Lu, Y. H. Chen and Y. H. Tai, High-stability oxygen sensor based on amorphous zinc tin oxide thin film transistor, *Appl. Phys. Lett.,* **100**, 262908 (2012).

[20] L. Li, Z. Lou and G. Shen, Flexible broadband image sensors with SnS quantum dots/Zn_2SnO_4 nanowires hybrid nanostructures, *Adv. Funct. Mater.,* **28** 1705389 (2018).

[21]B. Saturi, C. Abdullah and F. Y. Chik, Study on optical properties of tin oxide thin films at different annealing

temperatures, *Journal of Science and Technology*, 61-72 (2007).

[22] J. Biggs, J. Myers, J. Kufel, E. Ozer, S. Craske, A. Sou, C. Ramsdale, K. Williamson, R. Price and S. White, A natively flexible 32-bit Arm microprocessor, *Nature*, **595,** 532–536 (2021).

[23] J. Lindahl, J. Keller, O. Donzel-Gargand, P. Szaniawski, M. Edoff and T. Törndahl, Deposition temperature induced conduction band changes in zinc tin oxide buffer layers for Cu(In,Ga)Se2 solar cells, *Sol, Energy Mater. Sol. Cells,* **144,** 684 –690 (2016).

[24] S. Suresh and P. Jiban, Optical and electrical properties of nanocrystalline SnO_2 thin films synthesized by chemical bath deposition method, *Soft Nanoscience Letters*, **5** 55-64 (2015).

[25] V. G. Tamara, D. Mirosolar and U. P. M. Ashik, Overview of metal oxide nanostructures synthesis of inorganic nonmaterial's by spray pyrolysis, *JOSR Journal of Applied Physics,* **10**, 89-94 (2018).

[26] L. A. Isacc, A. Duta, A. Kriza, I. A. Enesca and M. Nanu, The growth of CuS thin films by Spray Pyrolysis, *Journal of Physics,* **61**, 477–481 (2007).

[27] A. Rovisc, R. Branquinho, J. Martins, M. J. Oliveira, D. Nunes, E. Fortunato, R. Martins and P. Barquinha, Seed-layer free zinc tin oxide tailored nanostructures for nanoelectronic applications: Effect of chemical parameters, *ACS Appl. Nano Mater.,* **1**, 3986–3997 (2018).

[28] M. B. Ali, R. Nasser, S. M. Alshahrani, H. A. Al-Shamiri, B. Elgammal and H. Elhouichet, Synthesis, characterization, and visible-light photocatalytic activity of transition metals doped ZTO nanoparticles, *Ceram. Int.*, **47,** 32882–32890 (2021).

[29] A. Rovisco, R. Branquinho, J. Deuermeier, T. S. Freire, E. Fortunato, R. Martins and P. Barquinha, Shape effect of zinc-tin oxide nanostructures on photodegradation of methylene blue and rhodamine B under UV and visible light, *ACS Appl. Nano Mater.,* **4**, 1149 –1161 (2021).

[30] H. I. Naşcu and V. Popescucus, Thin Films Obtained by Spray Pyrolysis, *Leonardo Electronic Journal of Practices and Technologies,* **4**, 22-29 (2004).

[31] M. S. Abdalla, A. S. F. Obada and M. Abdel-Aty, Von Neumann entropy and phase distribution of two mode parametric amplifier interacting with a single atom, *Annals of Physics,* **318**, 266–285 (2005).

[32] A. S. F Obada and M. Abdel-Aty, Influence of the stark shift and kerr-like medium on the evolution of field entropy and entanglement in two-photon processes, *Acta Physica Polonica B*, **31**, 589–599 (2000).

[33] M. Abdel-Aty, S. Furuichi and A. S. F. Obada, Entanglement degree of a nonlinear multiphoton Jaynes-Cummings model, *Journal of Optics B: Quantum and Semiclassical Optics,* **4,** 37–43 (2002).

[34] A. H. Abdel-Aty, H. Kadry, M. Zidan, E. A. Zanaty and M. Abdel-Aty, A quantum classification algorithm for classification incomplete patterns based on entanglement measure, *Journal of Intelligent and Fuzzy Systems,* **38**, 2817–2822 (2020).

[35] M. Zidan,, A. H. Abdel-Aty, A. Younes, I. El-khayat and M. Abdel-Aty, A novel algorithm based on entanglement measurement for improving speed of quantum algorithms, *Applied Mathematics and Information Sciences*, **12,** 265–269 (2018).